$$= \left(\frac{\partial H}{\partial u}\right)^i \eta(u_s{}^i - u^i) > 0, \quad t_1 < t < t_2 \quad (21)$$

which requires that the directional derivative of H^i be positive in the direction of the singular control point $u^i = u_s{}^i(t)$. The authors are not able to derive Equation (21) in a rigorous fashion. However, the requirement of Equation (21) will probably be met globally if the objective function possesses no stationary points or extrema in the region $u_{\min} < u < u_{\max}$ other than the maximum $u^i(t) = u_s{}^i(t)$. In other words, if the optimal solution contains the singular arc, then the equation should hold in the interval (t_1, t_2). Furthermore, if the combined modes solution is used as a terminal refinement scheme of successive approximation, only a local version of the requirement of Equation (21) needs consideration. In this case, the requirement should be met if the gradient process has progressed well before transition to the combined modes scheme.

In the experience obtained in the examples given in the companion paper (9) and in reference 8, it appears that the combined modes solution procedure converges to a solution which is a better approximation to the optimal solution than normally obtainable with a gradient method, as far as details of the optimal control time history $u(t)$ are concerned. Furthermore, it gives a faster convergence than the gradient method, when it is used as a terminal refinement scheme.

NOTATION

$\mathbf{B}(\mathbf{x})$ = coefficient matrix
$\mathbf{f}(\mathbf{x}, u)$ = vector state equation
$\mathbf{g}(\mathbf{x})$ = vector function in state equation
$g_0(\mathbf{x})$ = scalar function in the objective function
$G[\mathbf{x}(t_f)]$ = term in the objective function
$\mathbf{h}(\mathbf{x})$ = vector function in the state equation
$h_0(\mathbf{x})$ = scalar function in the objective function
H = Hamiltonian function
J = objective function
K = a positive constant
L = Lagrangian function
$\mathbf{m}(\mathbf{x})$ = matrix
$\mathbf{p}$ = adjoint vector
$\mathbf{q}(\mathbf{x})$ = vector function in Equation (9)
S_s = singular surface
t = time or other independent variable
u = control variable
u_s = singular control
$\mathbf{x}$ = state vector
β, γ = scalar functions in Equation (14)
$\epsilon, \epsilon', \epsilon''$ = small positive constants
η = small positive constant
$\phi(\mathbf{x}, \mathbf{p})$ = switching function
$\psi(\mathbf{x}, \mathbf{p})$ = scalar function in the Hamiltonian function

LITERATURE CITED

1. Athans, M., and P. L. Falb, "Optimal Control," McGraw Hill, New York (1966).
2. Dyson, D. C., and F. J. M. Horn, *J. Optimization Theory Appl.*, **1**, 40 (1967).
3. Goh, B. S., *J. SIAM Control*, **2**, No. 2 (1965).
4. Gunn, D. J., and W. J. Thomas, *Chem. Eng. Sci.*, **20**, 89 (1965).
5. Gunn, D. J., *ibid.*, **22**, 963 (1967).
6. Johnson, C. D., "Advances in Control System," C. T. Leondes, ed., Vol. 2, Academic Press, New York (1965).
7. Kelley, H. J., R. E. Kopp, and H. G. Moyer, "Topics in Optimization," G. Leitmann, ed., Academic Press, New York (1967).
8. Ko, D. Y. C., Ph.D. dissertation, Northwestern Univ., Evanston, Ill. (1969).
9. ———, and W. F. Stevens, *AIChE J.*, **17**, No. 1, 160 (1971).
10. Paynter, J. D., and S. G. Bankoff, *Can. J. Chem. Eng.*, **45**, 226 (1967).
11. Pontryagen, L. S., V. G. Boltyanski, R. V. Gambrelidge, and E. F. Mischenko. "The Mathematical Theory of Optimal Process," Interscience, New York (1962).
12. Seinfeld, J. H., and Leon Lapidus, *Chem. Eng. Sci.*, **23**, 1485-1499 (1968).
13. Siebenthal, C. D., and Rutherford Aris, *ibid.*, **19**, 729, 747 (1964).
14. Wonham, W. M., and C. D. Johnson, *Trans. Am. Soc. Mech. Engrs., J. Basic Eng.*, **86**, No. 1, 107 (1964).

Bubble Coalescence in Fluidized Beds: Comparison of Two Theories

ROLAND CLIFT and J. R. GRACE
McGill University, Montreal, Canada

Lin (*1*) presented an analysis of the motion of a pair of two-dimensional bubbles in vertical alignment based on Murray's (*3*) approximate equations for continuum flow of gas and particles in fluidized beds. Since these equations describe steady flow, the analysis is restricted to situations in which there is no relative motion between the bubbles. Therefore, Lin predicted the separation at which two bubbles have exactly the same velocity, assuming that the bubbles are exactly circular. He obtained the velocity potential describing particle flow relative to the bubbles and inserted this velocity potential into Murray's equations of motion to give an equation for the gas pressure. The condition that the gas pressure should be constant over the surface of each bubble in the vicinity of the nose then led to two independent equations, which were solved numerically to give the stable bubble spacing and rise velocity. The numerical predictions are shown in in Figures 1 and 2.

Clift and Grace (*2*) analyzed the motion of a bubble through a complex flow field resulting from any number of interacting bubbles in a fluidized bed. The analysis was based on Jackson's equations of motion (*4*), and it covered unsteady flow situations, since the effect of relative bubble motion on pressure was included (although smaller effects due to bubble acceleration were neglected). Each bubble was represented by a single doublet so that the resulting bubble boundaries were not exactly circular. It was shown that the velocity of a bubble in a fluidized bed may be approximated by adding its rise velocity in isolation to the velocity which the particulate phase would have at the position of the nose if the bubble were absent.

QUANTITATIVE COMPARISON

The theory of Clift and Grace covers unsteady motion of interacting bubbles in any orientation. If the distance between the centers of two bubbles in vertical alignment is d, then the theory predicts (*2*) that the relative velocity between the bubbles vanishes when

$$1 + \frac{s^{2.5}}{(D+1)^2} = s^{0.5} + \frac{1}{(D-s)^2} \quad (1)$$

where the bubble radii are, respectively, r_1 and r_2, s is the size ratio (r_2/r_1), and D is the dimensionless separation (d/r_1). Equation (1) defines a relationship between

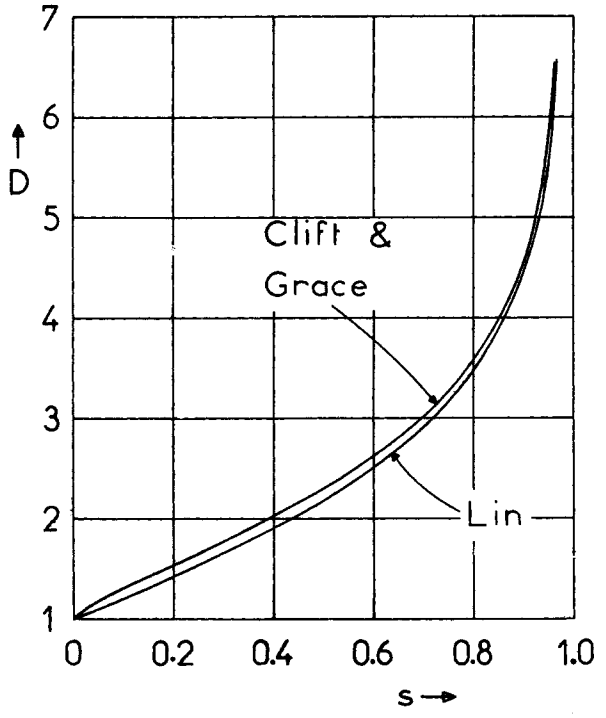

Fig. 1. Stable bubble spacings (D) as function of bubble size ratio(s).

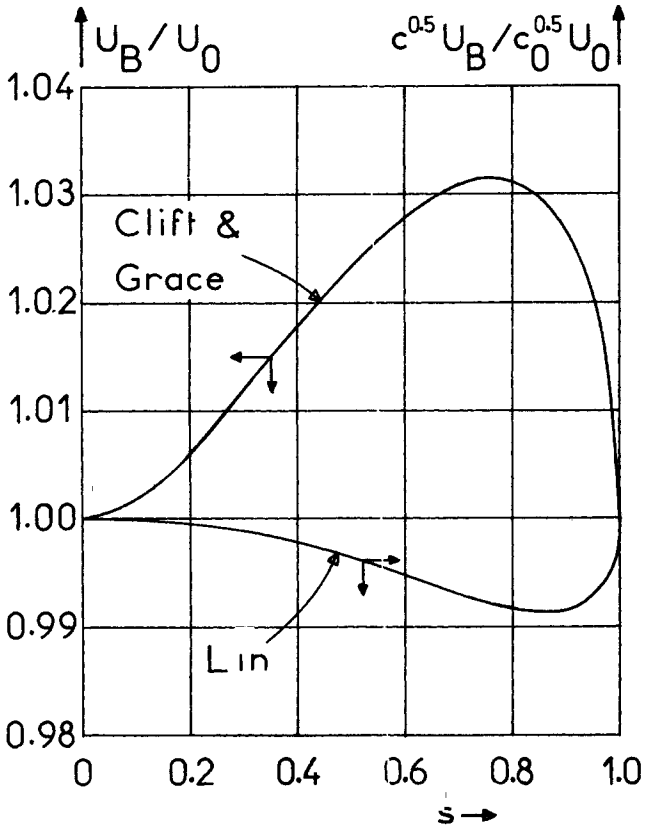

Fig. 2. Comparison of velocities of interacting and isolated bubbles, as function of bubble size ratio.

D and s, which is presented in Figure 1 along with the corresponding relationship from Lin's theory (*1*). Agreement between the two curves is remarkably good, showing that there is no significant difference between the exactly circular bubbles in Lin's analysis and the slightly distorted bubbles in the analysis of Clift and Grace. Both theories predict that the region below the curves corresponds to conditions which lead to coalescence, and both theories are consistent in this respect with available experimental results (*1, 2, 5*). It may also be noted that since both theories assume irrotational particulate-phase motion, both predict that bubbles of equal size ($s = 1$) in vertical alignment should always coalesce if the rise time is long enough.

Each of the theories also gives a relationship between the bubble size ratio s and the velocity U_B of a pair of bubbles with stable spacing. In Lin's theory, the bubble velocities cannot be separated from Murray's linearization constant c, so that it is only possible to calculate $c^{0.5}U_B/c_0^{0.5}U_0$ where c and c_0 are the linearization constants for interacting and isolated bubbles, respectively, and U_0 is the velocity which the front bubble would have in isolation. Lin's curve (*1*) for this ratio is plotted in Figure 2. The velocity ratio U_B/U_0 is predicted directly by the theory of Clift and Grace:

$$\frac{U_B}{U_0} = \frac{(D-s)^2\left[(D+1)^2 + s^{2.5}\right]}{(D-s)^2(D+1)^2 - s^2} \qquad (2)$$

This relationship is shown in Figure 2, where the value of D at stable spacing for given s has been determined from Equation (2). The theory of Clift and Grace predicts a velocity ratio greater than unity, and this is consistent with experimental results (*2, 5*) which show that, when two bubbles interact in a vertical line, the velocity of each is increased. Gabor (*6*) also predicted an increase in velocity for an infinite vertical chain of equal sized, equally spaced bubbles, based on an analysis very similar to Lin's. On the assumption that c and c_0 were approximately equal, Lin interpreted the curve of Figure 2 as suggesting that the velocity of the pair of bubbles U_B would be less than U_0. In fact, for Lin's theory to fit the experimental results, the constant c must be a function of bubble spacing and size ratio, and values of c/c_0 can be calculated from the curves of Figure 2. It should be noted that even the value c_0, appropriate to an isolated bubble, is a matter of some debate (*7, 8*).

CONCLUSION

When a bubble in a fluidized bed rises vertically behind a larger bubble, there is a critical spacing at which their velocities are identical. Two theories (*1, 2*) predict this critical spacing with good agreement. Doubt regarding the value of Murray's linearization constant c prevents the application of Lin's theory to predict the velocities of interacting bubbles. On the other hand, the simpler theory of Clift and Grace allows good quantitative predictions to be made of bubble velocities. Moreover, this theory can be applied to unsteady cases, and it has been extended to three-dimensional bubbles.

NOTATION

c = constant in Murray's modified Oseen linearization
c_0 = value of c for an isolated bubble
d = distance between centers of bubbles
D = dimensionless distance between bubble centers, d/r_1
r_1 = radius of leading bubble
r_2 = radius of rear bubble
s = bubble size ratio, r_2/r_1
U_B = velocity of a pair of bubbles with stable spacing
U_0 = velocity of an isolated bubble of radius r_1

LITERATURE CITED

1. Lin, S. P., *AIChE J.*, 16, 130 (1970).
2. Clift, Roland, and J. R. Grace, *Chem. Eng. Progr. Symposium Ser.*, to be published.

3. Murray, J. D., *J. Fluid Mech.*, **22**, 1, 57 (1965).
4. Jackson, R., *Trans. Inst. Chem. Engrs. (London)*, **41**, 22 (1963).
5. Clift, Roland, and J. R. Grace, paper presented at Am. Inst. Chem. Engrs. meeting, San Juan, Puerto Rico (May, 1970).
6. Gabor, J. D., *Ind. Eng. Chem. Fundamentals*, **8**, 84 (1969).
7. Rowe, P. N., and B. A. Partridge, *J. Fluid Mech.*, **23**, 583 (1965).
8. Collins, R., *Chem. Eng. Sci.*, **24**, 1291 (1969).

Vapor-Liquid Equilibria for Propane-Propylene

E. W. FUNK and J. M. PRAUSNITZ
University of California, Berkeley, California

Several authors have reported vapor-liquid equilibrium data for the propane-propylene system (*1* to *5*). We present here the results of data reduction as needed for computer calculations of vapor-liquid equilibria for wide ranges of temperature, pressure, and composition. Our results suggest that the relative volatility of propylene to propane at the propylene-rich end is appreciably lower than that estimated by Zdonik in 1958 (*7*). In view of the large commercial importance of propylene, our results may be of interest for optimum design of propylene plants.

Following the thermodynamic treatment of Prausnitz and Chueh (*6*), the equation of equilibrium is

$$\phi_i\, y_i\, P = \gamma_i^{(P0)}\, x_i\, f_i^{o(P0)} \exp \frac{\overline{v}_i P}{RT} \qquad (1)$$

In reducing the experimental data, the standard state fugacity for each component is the fugacity of the pure liquid at system temperature corrected to zero pressure. Equations for standard state fugacities for propane and for propylene are given in reference *6* (Appendix A).

Vapor-phase fugacity coefficients were calculated using a computer program (PHIMIX), and partial molar liquid volumes using a computer program (VOLPAR), as described in reference *6*.

The effect of liquid composition on activity coefficients is given by

$$\ln \gamma_1^{(P0)} = \alpha\, v_{c1}\, \Phi_2^2 \qquad (2)$$

and

$$\ln \gamma_2^{(P0)} = \alpha\, v_{c2}\, \Phi_1^2 \qquad (3)$$

where the volume fractions are defined by

$$\Phi_1 = \frac{x_1 v_{c1}}{x_1 v_{c1} + x_2 v_{c2}}; \quad \Phi_2 = \frac{x_2 v_{c2}}{x_1 v_{c1} + x_2 v_{c2}} \qquad (4)$$

Using the available experimental data together with a suitable computer program (SYMFIT) from reference *6*, we find that

$$\alpha^{1/2} = 0.305924 - 1.3273 \times 10^{-2} \left[\frac{T}{100}\right] - 1.7922 \times 10^{-3} \left[\frac{T}{100}\right]^2 - 1.431 \times 10^{-4} \left[\frac{T}{100}\right]^3 - 1.71 \times 10^{-5} \left[\frac{T}{100}\right]^4 \qquad (5)$$

Equation (5) represents the data over the temperature range 400 to 660°R. The maximum deviation between calculated and observed vapor-phase mole fractions is 0.005.

Figure 1 shows the relative volatility of propylene to propane as a function of pressure for several liquid-phase mole fractions. The relative volatility increases with decreasing pressure; however, this effect becomes very small at high concentrations of propylene. Therefore, in designing separation equipment for very pure propylene, little advantage is gained in operating at low pressures. This conclusion is different from that of Zdonik (*7*) who predicted a significant increase in relative volatility with a

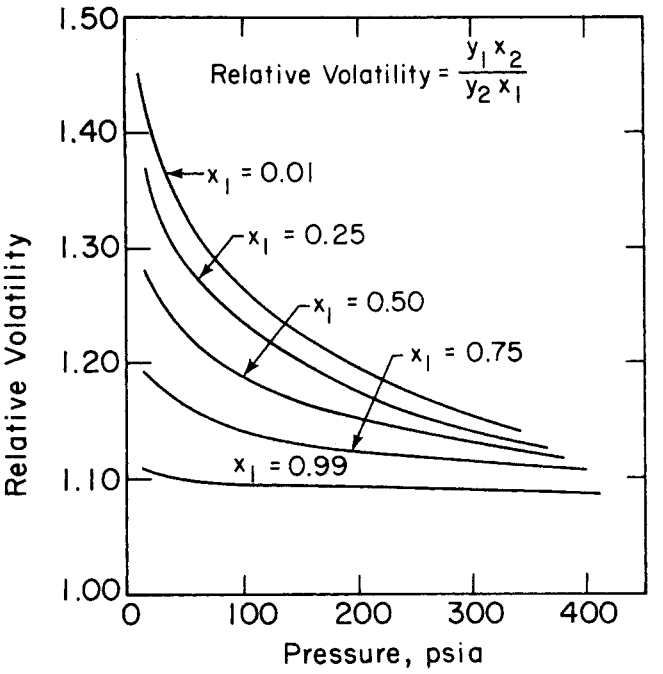

Fig. 1. Relative volatility of propylene (1) to propane (2) as a function of pressure at five liquid-phase mole fractions.